Heterojunction Ambipolar Organic Transistors Fabricated by a Two-Step Vacuum-Deposition Process

ARTICLE *in* ADVANCED FUNCTIONAL MATERIALS · APRIL 2006

Impact Factor: 11.81 · DOI: 10.1002/adfm.200500111

8 AUTHORS, INCLUDING:

Haibo Wang
Texas A&M International University
329 PUBLICATIONS **4,054** CITATIONS
SEE PROFILE

Jianwu Shi
Henan University
37 PUBLICATIONS **489** CITATIONS
SEE PROFILE

Dan Lei Yan
Institute of Microelectronics
26 PUBLICATIONS **293** CITATIONS
SEE PROFILE

FULL PAPER

ADVANCED FUNCTIONAL MATERIALS

DOI: 10.1002/adfm.200500111

Heterojunction Ambipolar Organic Transistors Fabricated by a Two-Step Vacuum-Deposition Process**

By *Jun Wang*, *Haibo Wang*, *Xuanjun Yan*, *Haichao Huang*, *Di Jin*, *Jianwu Shi*, *Yanhong Tang*, and *Donghang Yan**

Ambipolar organic field-effect transistors (OFETs) are produced, based on organic heterojunctions fabricated by a two-step vacuum-deposition process. Copper phthalocyanine (CuPc) deposited at a high temperature (250 °C) acts as the first (p-type component) layer, and hexadecafluorophthalocyaninatocopper (F_{16}CuPc) deposited at room temperature (25 °C) acts as the second (n-type component) layer. A heterojunction with an interpenetrating network is obtained as the active layer for the OFETs. These heterojunction devices display significant ambipolar charge transport with symmetric electron and hole mobilities of the order of 10^{-4} $cm^2 V^{-1} s^{-1}$ in air. Conductive channels are at the interface between the F_{16}CuPc and CuPc domains in the interpenetrating networks. Electrons are transported in the F_{16}CuPc regions, and holes in the CuPc regions. The molecular arrangement in the heterojunction is well ordered, resulting in a balance of the two carrier densities responsible for the ambipolar electrical characteristics. The thin-film morphology of the organic heterojunction with its interpenetrating network structure can be controlled well by the vacuum-deposition process. The structure of interpenetrating networks is similar to that of the bulk heterojunction used in organic photovoltaic cells, therefore, it may be helpful in understanding the process of charge collection in organic photovoltaic cells.

1. Introduction

Organic field-effect transistors (OFETs) have received extensive attention as basic switching elements, owing to their potential applications in inexpensive, large-area, and flexible consumer goods.[1–3] In contrast to conventional metal oxide semiconductor transistors based on silicon materials, ambipolar OFETs that are capable of operating in either the n- or p-channel region are a new challenge in fabricating complementary circuits.[4] The main advantages of complementary circuits are their high robustness, low power dissipation, and better noise immunity.[2] Currently, most ambipolar OFETs employ a heterostructure, interpenetrating network structure, or small-bandgap semiconductor, and can only be operated in a vacuum, because such devices slowly deteriorate when transferred into air.[4–9] Therefore, air-stable, ambipolar OFETs are crucial for practical applications. Recently, Babel et al. reported a type of air-stable, ambipolar OFET based on blending n-type poly(benzobisimidazobenzophenanthroline) (BBL) and p-type copper phthalocyanine (CuPc), which form an interpenetrating network.[10] The ambipolar electrical characteristics exhibit a strong dependence on the crystalline morphology and the nanoscale phase separation. However, it is difficult to control the morphology of the thin film by altering the thermal treatment and solvent.

We have fabricated air-stable, ambipolar OFETs based on an organic heterojunction. Two promising transistor materials, CuPc and hexadecafluorophthalocyaninatocopper (F_{16}CuPc), were used as the p- and n-type components, respectively, in the organic heterojunction. A two-step vacuum deposition process was carried out to prepare the heterojunction with an interpenetrating network structure; this is different from previous reports where the mixture of two components was achieved by spin-coating.[5,6] Different deposition parameters were utilized to control the morphology of the heterojunction thin film. X-ray diffraction (XRD) and atomic force microscopy (AFM) were used to study the crystalline structure and morphology of the thin film. All electrical characteristics of the OFETs were measured in air.

Organic heterojunctions have been widely applied in organic optoelectric devices, such as photovoltaic cells and photodetectors.[11,12] Furthermore, organic heterojunctions composed of α-hexathiophene (α-6T) or pentacene as the p-type component, and C_{60} or its derivative ((1-(3-methoxycarbonyl)propyl)-1-phenyl[6,6] C_{61}, PCBM) as the n-type component have been used to make ambipolar OFETs.[4,13,14] In these heterojunction OFETs, the material pair has to be selected carefully, taking into consideration their carrier mobilities and energy level alignment. However, most n-type materials often exhibit poor stability in air, which induces the deterioration of the electrical characteristics.[15,16] Fluorine or fluoroalkyl substituent com-

[*] Prof. D. Yan, Dr. J. Wang, H. Wang, X. Yan, H. Huang, D. Jin, J. Shi, Y. Tang
State Key Laboratory of Polymer Physics and Chemistry
Changchun Institute of Applied Chemistry
The Chinese Academy of Sciences
5625 Remin St., Changchun 130022 (P.R. China)
E-mail: yandh@ciac.jl.cn

[**] The work was financially supported by the Special Funds for Major State Basic Research Projects (2002CB613400) and the National Natural Science Foundation of China (90301008, 20474064).

ADVANCED FUNCTIONAL MATERIALS

pounds are a group of air-stable n-type materials owing to their electron-withdrawing capacity, which is sufficient to block moisture from penetrating through these films.[17,18] F_{16}CuPc, as proposed by Bao et al.,[17] is the first air-stable, n-type organic semiconductor to be utilized as the basic electronic element for organic logic circuits.[2] Herein, F_{16}CuPc was used as the n-type component in our experiments. CuPc, with a mobility of 10^{-2} $cm^2 V^{-1} s^{-1}$, was used as the p-type component.[19] This organic material pair was chosen for the heterojunction for two reasons. First, the two materials have closely comparable field-effect mobilities (of the order of 10^{-2} $cm^2 V^{-1} s^{-1}$), thus making it easier to achieve ambipolar characteristics.[13] Second, CuPc and F_{16}CuPc have identical molecular shapes, crystal packing, and grain size.[17,19] These characteristics will allow perfect crystal growth at the interface of the two organic semiconductors. Another consideration is that both CuPc and F_{16}CuPc have high chemical stability, and can be readily processed for practical applications. Recently, we reported an air-stable, ambipolar OFET fabricated using a heterojunction of CuPc and F_{16}CuPc in the layer structure. However, the two carrier mobilities were still low (of the order of 10^{-6} $cm^2 V^{-1} s^{-1}$).[20] In this paper, we propose a novel method to improve the ambipolar electrical characteristics of an OFET by controlling the morphology of the organic heterojunction.

It is well known that crystal grain size and molecular orientation have a strong influence on charge-carrier transportation.[21] Generally, a thin film grown on a substrate at a high substrate temperature (T_s) and a low growth rate will result in large crystals. In this case, the continuity of the thin film should be considered essential for high carrier mobility. This is especially important for OFETs, where the carrier transport is parallel to the substrate. Field-effect mobilities are highly dependent on the arrangement of the crystal and the order of the thin film at the interface near the gate insulator. In contrast, a film grown at a low T_s with a high deposition rate will comprise small crystals. Although good connections between crystal grains are obtained, the grain boundary will be increased, and result in a relatively low carrier mobility because of the high density of traps. Therefore, proper deposition parameters should be selected carefully to optimize the quality of the thin film. In a complementary method, Jackson's group has fabricated an improved OFET by using two layers of semiconductor deposited at different T_s values as the active layer.[22] This active layer was a stacked structure with the first layer of semiconductor deposited at a high T_s to obtain improved film ordering and the second semiconductor layer deposited at a lower T_s to fill in any voids and improve film continuity. Based on these considerations, we prepared an organic heterojunction thin film with an interpenetrating network structure, deposited at different T_s values, to obtain ambipolar electrical characteristics.

The structure of the OFET heterojunction is shown in Figure 1a. CuPc was deposited as the first active layer on top of the gate insulator, F16CuPc was deposited as the second active layer on top of the source/drain electrodes and CuPc. This device structure is defined as a sandwich configuration (SC), and gives improved carrier injection.[23] The schematic energy levels for the interpenetrating network of CuPc and F16CuPc are shown in Figure 1b (for simplicity, band bending is ruled out). The highest occupied molecular orbital (HOMO) of CuPc is 5.0 eV, which matches the work function of gold (5.1 eV), resulting in Ohmic hole injection to CuPc (the interface dipolar (the difference of the vacuum energy level between the metal and organic semiconductors) is neglected).[24] On the other hand, there is a new, 0.3 eV electron-injection barrier, due to the lowest unoccupied molecular orbital (LUMO) of F_{16}CuPc (4.8 eV).[25] However, the injection barrier displays a strong dependence on the electric field, which can be reduced by increasing the gate and drain voltages in OFETs. In addition, the small injection barrier can also be overcome by charge tunneling. Therefore, the CuPc/F_{16}CuPc pair is a good choice for providing ambipolar electrical characteristics.

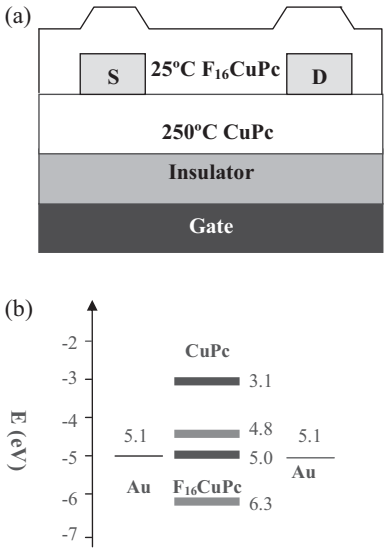

Figure 1. a) Schematic cross section of the sandwich configuration (SC)OFETs used in this study; S = source D = drain electrode. b) Energy level diagram of the interpenetrating network of CuPc and F_{16}CuPc, and alignment with Au as the S/D electrodes.

2. Results and Discussion

The first layer of CuPc was deposited on a substrate held at $T_s = 250\,^{\circ}C$, in order to obtain large crystals and form a CuPc matrix. The thickness of the film was controlled by building up separate, single layers, and was found to be approximately 5 nm thick. Because the electrical properties of 5 nm thick CuPc are difficulty to measure, owing to the low coverage of the substrate, we also prepared a 25 nm thick CuPc thin film by same process. An AFM image of the 25 nm thick CuPc vacuum deposited at 250 °C is shown in Figure 2a. The polycrystalline thin film consists of approximately 500 nm long, discontinuous crystal grains. The multilayer crystal-grain stacking displays the Vollmer–Weber (islands starting at the first monolayer) growth mode. Some voids are observed in the film deposited at high T_s. These voids provide locations upon which

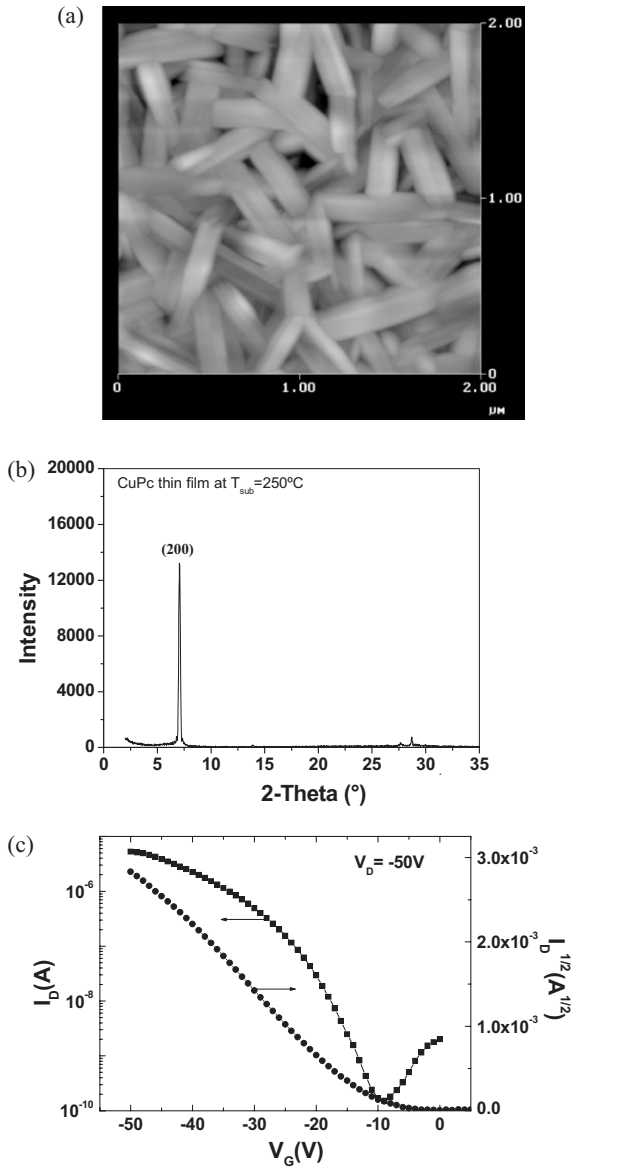

Figure 2. a) AFM image of a 25 nm thick CuPc film grown on a SiO_2 substrate at 250 °C. b) XRD pattern of a 25 nm thick CuPc film grown on a SiO_2 substrate at 250 °C. c) Transfer curves of OFETs based on a single layer of CuPc thin film grown under the same conditions.

the second layer can grow. XRD measurements (Fig. 2b) indicate that the CuPc thin film is highly crystalline. A sharp diffraction peak at $2\theta \approx 7.06°$, corresponding to an interplanar distance of 12.5 Å, is observed, which is the result of diffraction from the (200) lattice plane separated (approximately) by the interstacking distance. These results indicate that the CuPc thin film adopts the metastable α-phase, and the trace of the herringbone pattern is parallel to the substrate. This arrangement is beneficial to charge transportation at the interface of the source/drain contacts in OFETs.[19]

Top-contact (TC)OFETs based on single-layer CuPc were fabricated. The transfer curves from which the field-effect mobility (0.042 $cm^2 V^{-1} s^{-1}$) was extracted are shown in Figure 2c. This is a several-fold increase in mobility compared with previous reports,[19] and is due to the very careful control exercised in the preparation of the CuPc thin film. The deposition rate was kept at a relatively low level (0.1 Å s^{-1}) to ensure the CuPc molecules fully diffused on the substrate, in order to gain in crystal grain size.

Figure 3a shows the AFM image of the second layer, a 25 nm thick F_{16}CuPc thin film deposited at room temperature after a slow-cooling process. The detailed deposition process is described in the Experimental Section. The image reveals the film consists of numerous small grains covering the whole substrate. The morphology of a thin film of F_{16}CuPc is related to

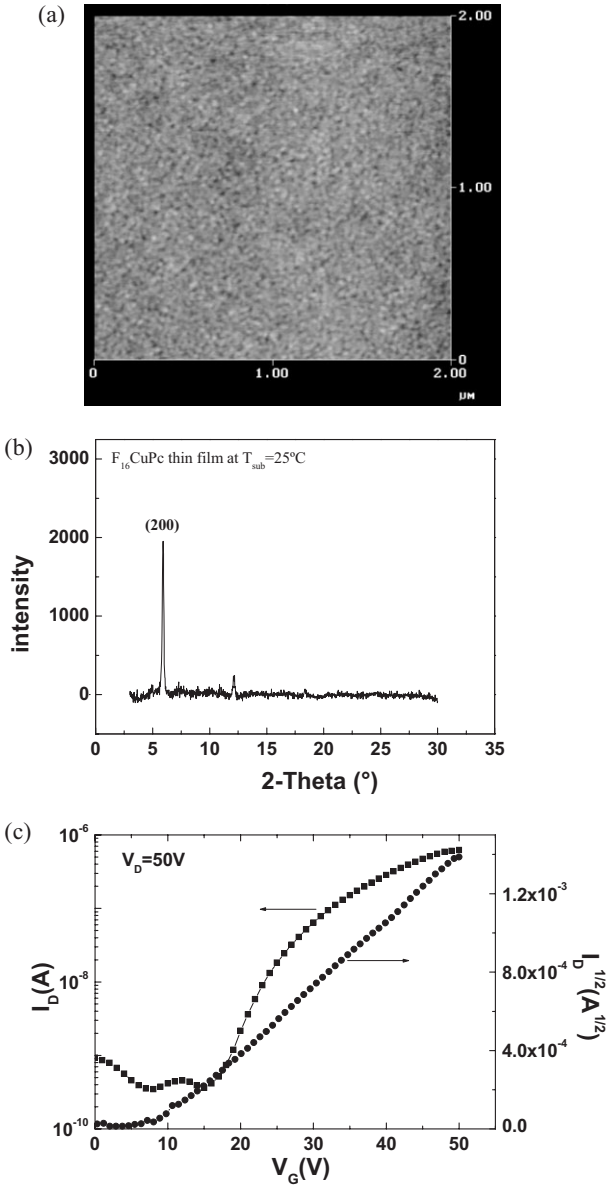

Figure 3. a) AFM image of the second layer of a 25 nm thick F_{16}CuPc film grown on a SiO_2 substrate at 25 °C. b) X-ray diffraction pattern of the second layer of a 25 nm thick F_{16}CuPc film grown on a SiO_2 substrate at 25 °C. c) Transfer curves of OFETs based on a single layer of F_{16}CuPc thin film fabricated under the same conditions.

ADVANCED FUNCTIONAL MATERIALS

the nucleation density, growth rate, and the surface energy provided from the substrate.[17] Figure 3b shows the XRD measurements for F_{16}CuPc, which indicate that the F_{16}CuPc thin film on SiO_2 is highly crystalline with a sharp diffraction peak at $2\theta \approx 5.901°$, corresponding to an interplanar distance of 14.96 Å, which is the result of diffraction from the (200) lattice plane separated (approximately) by the interstacking distance.[17] This crystalline arrangement and stacking is similar to the growth mode for CuPc. In this case, the TCOFETs were fabricated based on single-layer F_{16}CuPc. The transfer curves, from which a field-effect mobility of 0.0076 $cm^2 V^{-1} s^{-1}$ was extracted, are shown in Figure 3c. Although the value is slightly smaller than the best results for F_{16}CuPc-based OFETs under optimized conditions,[17] here we have simply taken advantage of the numerous small F_{16}CuPc crystal grains filling the (large) network of CuPc to prepare the interpenetrating heterojunction thin film.

The AFM image of the topology of the heterojunction of CuPc/F_{16}CuPc described above is shown in Figure 4a. The CuPc thin film with large crystal grains (first active layer), and the F_{16}CuPc film with small crystals (second active layer) can be seen clearly. The two-layer thin film forms an interpenetrating network structure, in which the CuPc thin film with large grains as the matrix is filled by numerous small grains of F_{16}CuPc. Therefore, two conducting channels consisting of p-type CuPc and n-type F_{16}CuPc are formed in the heterojunction. The XRD pattern of the heterojunction thin film is shown in Figure 4b. It consists of two diffraction peaks at $2\theta \approx 6.299°$, 6.84°, corresponding to the F_{16}CuPc (200) and CuPc (200) lattice planes.[17,19] The two peaks are identified from the interplanar distances (12.5 Å for CuPc, and 14.01 Å for F_{16}CuPc). These results indicated the thin film is still highly crystalline, with a herringbone pattern in an upright configuration on the SiO_2 substrate.

All OFETs were measured in air with a standard metal oxide semiconductor (MOS)FET model. Figure 5 shows the output characteristics of the heterojunction OFET based on the CuPc/F_{16}CuPc interpenetrating network structure described above, in which typical ambipolar electrical characteristics were clearly observed in a single device. Two successive measurements were carried out by applying various positive and negative gate voltages (V_G) and drain voltages (V_D) with respect to

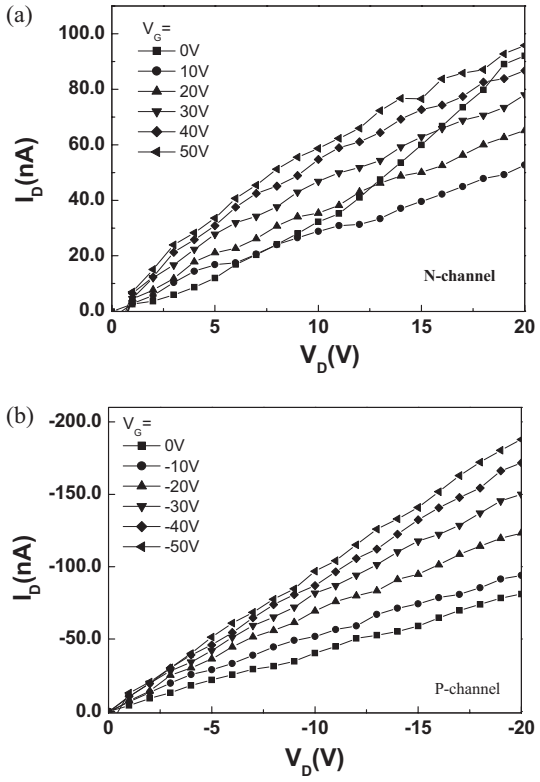

Figure 5. Output characteristics of the CuPc/F_{16}CuPc-based heterojunction ambipolar field-effect transistor: a) n-channel mode from gate–source (V_G) = 0 V to 50 V; b) p-channel mode from V_G = 0 to –50 V.

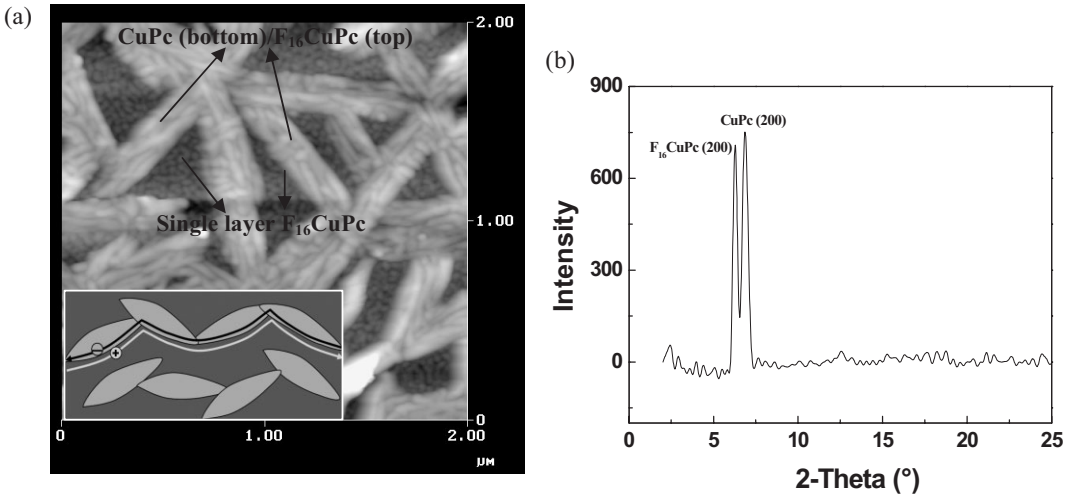

Figure 4. The film characteristics of the interpenetrating CuPc/F_{16}CuPc heterojunction. The CuPc and F_{16}CuPc layers are 5 and 25 nm thick, respectively. The CuPc film was grown at 250 °C, and the F_{16}CuPc at 25 °C. a) AFM image. The inset is a schematic illustration of the electron- and hole-transport characteristics in the organic heterojunction; b) X-ray diffraction pattern.

electron-enhancement and hole-enhancement modes. When a positive V_G was applied, electrons accumulated at the $F_{16}CuPc/SiO_2$ interface. An electron channel formed in the $F_{16}CuPc$ layer. Typical output curves of the n-channel transistor, operated for positive V_D and V_G, are shown in Figure 5a. At V_G = 0 V, an exponential increase in the current is observed with increasing V_D, owing to hole-injection from the drain contact. This result is consistent with those of previously reported ambipolar OFETs.[4–9]

When negative gate voltages were applied, holes were induced at the interface between CuPc and SiO_2. A hole channel was formed in the CuPc layer. As a result, the drain current increases almost linearly with increasing V_D at a constant V_G, which indicates an increase in the number of induced holes with increased gate voltage. No apparent saturation regime was observed (Fig. 5b). This is attributed to the existence of electrons that give rise to the development of a depletion zone near the drain contact.[26] The off-state current of these heterojunction OFETs is relatively high (approximately 2.5×10^{-7} A), whereas devices using a single-component phthalocyanine compound are usually of the order of $\sim 10^{-10}$–10^{-9} A. This high current property can be attributed to the weak charge-transfer process from $F_{16}CuPc$ to CuPc: similar behavior has been observed for the $F_{16}ZnPc/ZnPc$ pair.[27]

Figure 6 shows the transfer characteristics of heterojunction OFETs based on the $CuPc/F_{16}CuPc$ interpenetrating network structure. Figure 6 is composed of two curves with various V_D and V_G values. For $V_D = -50$ V, the continuously increasing drain current originates from hole charges when $V_G < -5$ V. On the other hand, the increasing drain current may be responsible for electron transport when the applied $V_G > -5$ V (here, for simplicity this voltage is defined as the switch-on voltage, V_S). The field-effect mobility for the hole current is found to be in the range ~ 3.8–7.8×10^{-4} $cm^2 V^{-1} s^{-1}$ from these data and a further three experiments. Similar electrical behavior can be seen for the electron current. For $V_D = 50$ V, the electron-enhancement mode is observed at applied $V_G > 36$ V. In contrast to the hole current, the V_S is relatively high, which is due to the injection barrier between $F_{16}CuPc$ and Au. A field-effect mobility for the electron current ranging from ~ 1.4 to 4.6×10^{-4} $cm^2 V^{-1} s^{-1}$ was extracted. Symmetric electron and hole mobilities were obtained, the origins of which are the morphology of the heterojunction fabricated in a controlled, two-step deposition process. The transport behavior of electrons and holes in a $CuPc/F_{16}CuPc$ heterojunction is illustrated in the inset of Figure 4a. Conductive channels for electrons and holes are formed at the $CuPc/F_{16}CuPc$ interface under various gate voltages. Electrons and holes are transported in $F_{16}CuPc$ and CuPc, respectively, which results in ambipolar electrical transport characteristics. The transport behavior of the electrons and holes is similar to that in bulk heterojunction in organic photovoltaic cells, and optimization of this behavior is a key issue nowadays. These devices are very stable in air (note

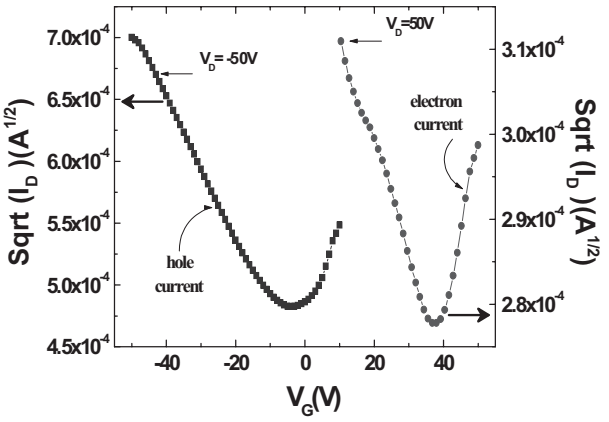

Figure 6. Transfer characteristics of the $CuPc/F_{16}CuPc$-based heterojunction field-effect transistor under negative and positive gate bias. Hole-enhancement mode and electron-enhancement mode are shown in the plot.

that all measurements were performed in ambient conditions). The ambipolar electrical characteristics did not degrade over a week, without any intentional protection. This stability is related to the fluorine atoms of $F_{16}CuPc$, which protect the film from the air. More importantly, a new fabrication process for preparing organic heterojunctions with an interpenetrating network structure has been provided.

Table 1 shows the field-effect mobilities with different T_s and thicknesses of the active layer in heterojunction OFETs. We can see that the electrical characteristics of heterojunction OFETs show a dependence on the proportion of the thickness of the two semiconductors. When the thickness of CuPc is decreased to 2.5 nm, the hole mobility decreases, while the electron mobility increases. On increasing the thickness of CuPc to 15 nm, the ambipolar character disappears and the unipolar hole mobility increases by almost two orders of magnitude.

It is known that the bulk charges in an organic semiconductor thin film can be described approximately as qn_0d_s, where q is the elementary charge, n_0 is the density of the majority car-

Table 1. Field-effect mobilities of heterojunction devices fabricated under various conditions. Values are reported as a range, because more than three devices were used to measure each condition. The extraction method of these mobilities is described in the Experimental section.

CuPc deposited under various conditions	$F_{16}CuPc$ deposited under various conditions	Hole mobility [$cm^2 V^{-1} s^{-1}$]	Electron mobility [$cm^2 V^{-1} s^{-1}$]
T_s = 250 °C thickness = 5 nm	T_s = 25 °C thickness = 25 nm	~ 3.8–7.8×10^{-4}	~ 1.4–4.6×10^{-4}
T_s = 250 °C thickness = 2.5 nm	T_s = 25 °C thickness = 25 nm	~ 1.2–4.8×10^{-5}	~ 5.1–8.3×10^{-4}
T_s = 250 °C thickness = 15 nm	T_s = 25 °C thickness = 25 nm	2.5×10^{-2} (unipolar)	No observation
T_s = 250 °C thickness = 2 nm	T_s = 250 °C thickness = 10 nm	~ 1.3–5.2×10^{-6}	~ 5.1–9.4×10^{-5}
T_s = 250 °C thickness = 3 nm	T_s = 250 °C thickness = 10 nm	2.2×10^{-2} (unipolar)	No observation
T_s = 250 °C thickness = 5 nm	T_s = 250 °C thickness = 10 nm	2.0×10^{-2} (unipolar)	No observation

ADVANCED FUNCTIONAL MATERIALS

rier of the semiconductor, and d_s is the thickness of the semiconductor.[28] Therefore, the quantity of accumulated holes near the insulator under a constant gate voltage increases with increasing CuPc thickness, inducing a dominant hole current and screening the electron current. On the other hand, in our experiments, CuPc can be seen as a TC device and F_{16}CuPc as the bottom contact (BC) device. In this case, the contact resistance for Au/F_{16}CuPc is larger than that of Au/CuPc. (The contact resistance of a TC device is generally smaller than that of a BC device.) This results in unipolar electrical characteristics, where only hole current is displayed. Therefore, the thickness of the heterojunction material pair may be used to tune the two types of carrier density to obtain ambipolar OFETs. Generally, in heterojunction OFETs, the thickness of the second semiconductor layer (F_{16}CuPc in our experiments) is several times larger than that of the first semiconductor layer (CuPc) for ambipolar charge transport.

It is interesting that ambipolar electrical characteristics were observed for the heterojunction OFET with 2 nm thick CuPc and 10 nm thick F_{16}CuPc at the same T_s (250 °C, Table 1). Although both semiconductor layers were deposited at a high T_s, a suitable ratio of thicknesses is also necessary to induce ambipolar transistor characteristics.[20] Tuning the thickness ratio of the two semiconductors results in a balance of the two carrier densities for ambipolar electrical characteristics. However, the ambipolar mobilities in these heterojunction devices were one order of magnitude smaller than those of devices based on the heterojunction with an interpenetrating network (see Table 1). Therefore, the use of an interpenetrating, organic heterojunction is an effective method for fabricating ambipolar OFETs with improved performance. In particular, for low-mobility organic semiconductors (smaller than 10^{-3} $cm^2 V^{-1} s^{-1}$), the interpenetrating structure is crucial for ambipolar electrical characteristics. On further increasing the thickness of CuPc, only the hole current was present. In this case, the device operates in unipolar mode, with hole mobilities (10^{-2} $cm^2 V^{-1} s^{-1}$) approaching those of single-component devices.

In our experiments, the pair of p–n materials was carefully selected for the heterojunction by considering the energy alignment and material properties. The energy alignment between the heterojunction and source/drain contacts must be considered in order to lower the injection barrier for both electrons and holes as much as possible. Additionally, the materials' stability in air and their growth manner should also be considered. CuPc and F_{16}CuPc have similar crystal stackings, which may induce good electrical contact between the two layers, as if there were a continuous crystal growth at the interface—as would be found for a single material. Similar stacking interactions have been reported in other organic systems, such as benzene/perfluorobenzene and pentacene/perfluoropentacene.[13,29] Consideration of these factors is very useful for the preparation of organic heterojunctions, since they will contribute to the ambipolar electrical characteristics. In a previous report, the mobilities for ambipolar OFETs based on an interpenetrating network structure fabricated by a solution-process are lower by almost two or three orders of magnitude than single-component devices, which is due to the disorder of the active layer. Both the electron and hole mobilities reported previously are unsymmetrical, and of the order of 10^{-6}–10^{-4} $cm^2 V^{-1} s^{-1}$. Here, we have prepared a heterojunction with an interpenetrating network structure by a vacuum vapor deposition. This method produces a well-ordered heterojunction thin film, which improves the ambipolar electrical characteristics. Very high, balanced hole (7.8×10^{-4} $cm^2 V^{-1} s^{-1}$) and electron (4.6×10^{-4} $cm^2 V^{-1} s^{-1}$) mobilities measured in air were obtained. To the best of our knowledge, this is the first report of a heterojunction ambipolar transistor with an interpenetrating network structure fabricated by vacuum deposition.

3. Conclusions

Air-stable, ambipolar OFETs were fabricated based on a heterojunction of CuPc/F_{16}CuPc. A 5 nm CuPc thin film was deposited first as the p-type component on a substrate held at 250 °C; a 25 nm F_{16}CuPc thin film was deposited second as the n-type component on a substrate held at room temperature (25 °C). This heterojunction, with its interpenetrating network structure, was obtained by carefully controlling the morphology of these two components. These transistors display typical ambipolar charge transport, with symmetric electron and hole mobilities of the order of 10^{-4} $cm^2 V^{-1} s^{-1}$. This is attributed to the optimized morphology of the two-component system. Consequently, current research will also provide a simple path to the fabrication of air-stable, ambipolar OFETs, which will be good candidates for organic complementary circuits. The understanding of ambipolar transport behavior in the OFETs is also helpful for fabricating optimized bulk heterojunctions, which is a key issue for improving the conversion efficiency of organic photovoltaic cells.

4. Experimental

Device Fabrication and Measurements: The source samples of CuPc and F_{16}CuPc were purchased from Aldrich (USA) and purified three times by gradient sublimation before use. CuPc and F_{16}CuPc were deposited by vacuum deposition at a reduced pressure of 10^{-5} Pa. Films were grown at various T_s and thicknesses. A quartz oscillator was used to monitor the thickness of the thin films. Films with a high T_s (250 °C) were grown at an average rate of 0.1 Å s^{-1}, and films with a low T_s (25 °C) were grown at an average rate of 1 Å s^{-1}. n-Type doped Si wafers (0.01–0.015 Ω cm) were used as the gate electrode and substrate. A 1500 Å layer of SiO_2 covering the surface of a Si wafer (deposited by thermal oxidation) acted as the gate insulator. Then, 40 nm Au source/drain electrodes were fabricated through a shadow mask by thermal evaporation. The defined channel width (W) and length (L) were 1300 and 180 μm, respectively. The electrical characteristics of these heterojunction OFETs were measured using two Keithley 236 source measurement units under ambient conditions. The field-effect mobilities were extracted from the saturation region. By fitting curves to plots of $I_D^{1/2}$ (the square root of source-drain current) versus V_G, slopes were obtained and used to determine the mobilities, using Equation 1

$$I_D^{1/2} = \sqrt{\frac{W}{2L}\mu C_i (V_G - V_T)} \quad (1)$$

where C_i is the capacitance of gate insulator.

XRD Measurements: Thin-film patterns were taken on a Rigaku D/max 2500 W 18 kW system with a Cu Kα source ($\lambda = 1.54056$ Å).

AFM Measurements: Films were imaged on a Digital Instruments Multimode (AFMNS3A/BIOSCOPE) in air using tapping mode.

Received: February 25, 2005
Final version: August 16, 2005
Published online: February 16, 2006

[1] H. Edzer, A. Huitema, G. H. Gelinck, J. Bas, P. H. Van Der Putten, K. E. Kuijk, K. M. Hart, E. Cantatore, D. M. De Leeuw, *Adv. Mater.* **2002**, *14*, 1201.
[2] B. Crone, A. Dodabalapur, Y. Y. Lin, R. W. Filas, Z. Bao, A. Laduca, R. Sarpeshkar, H. E. Katz, W. Li, *Nature* **2000**, *403*, 521.
[3] C. D. Dimitrakopoulos, P. R. L. Malenfant, *Adv. Mater.* **2002**, *14*, 99.
[4] A. Dodabalapur, H. E. Katz, L. Torsi, R. C. Haddon, *Science* **1995**, *269*, 1560.
[5] K. Tada, H. Harada, K. Yoshino, *Jpn. J. Appl. Phys., Part 2* **1996**, *35*, L944.
[6] E. J. Meijer, D. W. de Leeuw, S. Setayesh, E. van Veenendaal, B.-H. Huisman, P. W. M. Blom, J. C. Hummelen, U. Scherf, T. M. Klapwijk, *Nat. Mater.* **2003**, *2*, 678.
[7] C. Rost, D. J. Gundlach, S. Karg, W. Riess, *J. Appl. Phys.* **2004**, *95*, 5782.
[8] R. J. Chesterfield, C. R. Newman, T. M. Pappenfus, P. C. Ewbank, M. H. Haukaas, K. R. Mann, L. L. Miller, C. D. Frisbie, *Adv. Mater.* **2003**, *15*, 1278.
[9] M. A. Correa-Duarte, N. Sobal, L. M. Liz-Marzan, M. Giersig, *Adv. Mater.* **2004**, *16*, 2174.
[10] A. Babel, J. D. Wind, S. A. Jenekhe, *Adv. Funct. Mater.* **2004**, *14*, 891.
[11] J. J. M. Halls, C. A. Walsh, N. C. Greenham, E. A. Marseglia, R. H. Friend, S. C. Moratti, A. B. Holmes, *Nature* **1995**, *376*, 498.
[12] P. Schilinsky, C. Waldauf, C. J. Brabec, *Appl. Phys. Lett.* **2002**, *81*, 3885.
[13] Y. Sakamoto, T. Suzuki, M. Kobayashi, Y. Gao, Y. Fukai, Y. Inoue, F. Sato, S. Tokito, *J. Am. Chem. Soc.* **2004**, *126*, 8138.
[14] E. Kuwahara, Y. Kubozono, T. Hosokawa, T. Nagano, K. Masunari, A. Fujiwara, *Appl. Phys. Lett.* **2004**, *85*, 4765.
[15] S. Kobayashi, T. Takenobu, S. Mori, A. Fujiwara, Y. Iwasa, *Appl. Phys. Lett.* **2003**, *82*, 4581.
[16] P. R. L. Malenfant, C. D. Dimitrakopoulos, J. D. Gelorme, L. L. Kosbar, T. O. Graham, A. Curioni W. Andreoni, *Appl. Phys. Lett.* **2002**, *80*, 2517.
[17] Z. Bao, A. J. Lovinger, J. Brown, *J. Am. Chem. Soc.* **1998**, *120*, 207.
[18] A. Facchetti, M. Mushrush, H. E. Katz, T. J. Marks, *Adv. Mater.* **2003**, *15*, 33.
[19] Z. Bao, A. J. Lovinger, A. Dodabalapur, *Appl. Phys. Lett.* **1996**, *69*, 3066.
[20] J. Wang, H. B. Wang, X. J. Yan, H. C. Huang, D. H. Yan, *Chem. Phys. Lett.* **2005**, *407*, 87.
[21] X. L. Chen, A. J. Lovinger, Z. Bao, J. Sapjeta, *Chem. Mater.* **2001**, *13*, 1341.
[22] Y. Y. Lin, D. J. Gundlach, S. F. Nelson, T. N. Jackson, *IEEE Electron. Device Lett.* **1997**, *18*, 606.
[23] J. Zhang, J. Wang, H. B. Wang, D. H. Yan, *Appl. Phys. Lett.* **2004**, *84*, 142.
[24] H. Peisert, M. Knupfer, T. Schwieger, J. M. Auerhammer, M. S. Golden, J. Fink, *J. Appl. Phys.* **2002**, *91*, 4872.
[25] C. Shen, A. Kahn, *J. Appl. Phys.* **2001**, *90*, 4549.
[26] A. R. Brown, C. P. Jarrett, D. M. de Leeuw, M. Matters, *Synth. Met.* **1997**, *88*, 37.
[27] D. Schlettwein, K. Hesse, N. E. Gruhn, P. A. Lee, K. W. Nebeny, N. R. Armstrong, *J. Phys. Chem. B* **2001**, *105*, 4791.
[28] G. Horowitz, in *Semiconducting Polymers* (Eds: G. Hadziioannou, P. F. van Hutten), Wiley-VCH, Weinheim, Germany **2000**, p. 463.
[29] E. A. Meyer, R. K. Castellano, F. Diederich, *Angew. Chem. Int. Ed.* **2003**, *42*, 1210.